

# A measurement of large-scale peculiar velocities of clusters of galaxies: results and cosmological implications.

A. Kashlinsky<sup>1</sup>, F. Atrio-Barandela<sup>2</sup>, D. Kocevski<sup>3</sup>, H. Ebeling<sup>4</sup>

## ABSTRACT

Peculiar velocities of clusters of galaxies can be measured by studying the fluctuations in the cosmic microwave background (CMB) generated by the scattering of the microwave photons by the hot X-ray emitting gas inside clusters. While for individual clusters such measurements result in large errors, a large statistical sample of clusters allows one to study cumulative quantities dominated by the overall bulk flow of the sample with the statistical errors integrating down. We present results from such a measurement using the largest all-sky X-ray cluster catalog combined to date and the 3-year WMAP CMB data. We find a strong and coherent bulk flow on scales out to at least  $\gtrsim 300h^{-1}\text{Mpc}$ , the limit of our catalog. This flow is difficult to explain by gravitational evolution within the framework of the concordance  $\Lambda\text{CDM}$  model and may be indicative of the tilt exerted across the entire current horizon by far-away pre-inflationary inhomogeneities.

*Subject headings:* cosmology: observations - cosmic microwave background - early Universe - large-scale structure of universe

In the gravitational-instability picture peculiar velocities probe directly the peculiar gravitational potential [e.g. Kashlinsky & Jones 1991, Strauss & Willick 1995]. Inflation-based theories, such as the concordance  $\Lambda\text{CDM}$  model, predict that, on scales outside the horizon during the radiation-dominated era, the peculiar density field remained in the Harrison-Zeldovich regime set during inflationary epoch and on these scales, the peculiar bulk velocity due to gravitational instability should decrease as  $V_{\text{rms}} \propto r^{-1}$  and be quite small. Peculiar velocities can be obtained from the kinematic SZ (KSZ) effect on the CMB

---

<sup>1</sup>SSAI and Observational Cosmology Laboratory, Code 665, Goddard Space Flight Center, Greenbelt MD 20771; e-mail: alexander.kashlinsky@nasa.gov

<sup>2</sup>Fisica Teorica, University of Salamanca, 37008 Salamanca, Spain

<sup>3</sup>Department of Physics, University of California at Davis, 1 Shields Avenue, Davis, CA 95616

<sup>4</sup>Institute for Astronomy, University of Hawaii, 2680 Woodlawn Drive, Honolulu, HI 96822

photons by the hot gas in clusters of galaxies [e.g. Birkinshaw 1999]. For each cluster the KSZ term is small, but measuring a quantity derived from CMB data for a sizeable ensemble of many clusters moving at a coherent bulk flow can, however, overcome this limitation. As proposed by Kashlinsky & Atrio-Barandela (2000, KA-B), such a measurement will be dominated by the bulk-flow KSZ component with other contributions integrating down. This quantity, *the dipole of the cumulative CMB temperature field evaluated at cluster positions*, is used in this investigation of the 3-year WMAP data together with the largest X-ray selected sample of clusters to date to obtain the best measurement yet of bulk flows out to scales of  $\gtrsim 300h^{-1}\text{Mpc}$ . Technical details of the analysis are given in the companion paper (Kashlinsky et al 2008 - KA-BKE). Our findings imply that the Universe has a surprisingly coherent bulk motion out to at least  $\simeq 300h^{-1}\text{Mpc}$  and with a fairly high amplitude of  $\gtrsim 600\text{-}1000\text{ km/sec}$ , necessary to produce the measured amplitude of the dipole signal of  $\simeq 2\text{-}3\mu\text{K}$ . Such a motion is difficult to account for by gravitational instability within the framework of the standard concordance  $\Lambda\text{CDM}$  cosmology but could be explained by the gravitational pull of pre-inflationary remnants located well outside the present-day horizon.

## 1. Method and data preparation

If a cluster at angular position  $\vec{y}$  has the line-of-sight velocity  $v$  with respect to the CMB, the CMB fluctuation caused by the SZ effect at frequency  $\nu$  at this position will be  $\delta_\nu(\vec{y}) = \delta_{\text{TSZ}}(\vec{y})G(\nu) + \delta_{\text{KSZ}}(\vec{y})H(\nu)$ , with  $\delta_{\text{TSZ}} = \tau T_X / T_{e,\text{ann}}$  and  $\delta_{\text{KSZ}} = \tau v / c$ . Here  $G(\nu) \simeq -1.85$  to  $-1.25$  and  $H(\nu) \simeq 1$  over the WMAP frequencies,  $\tau$  is the projected optical depth due to Compton scattering,  $T_X$  is the temperature of the intra-cluster gas, and  $k_B T_{e,\text{ann}} = 511\text{ keV}$ . Averaged over many isotropically distributed clusters moving at a significant bulk velocity with respect to the CMB, the dipole from the kinematic term will dominate, allowing a measurement of  $V_{\text{bulk}}$ . Thus KA-B suggested measuring the dipole component of  $\delta_\nu(\vec{y})$ .

We use a normalized notation for the dipole power  $C_1$ , such that a coherent motion at velocity  $V_{\text{bulk}}$  leads to  $C_{1,\text{kin}} = T_{\text{CMB}}^2 \langle \tau \rangle^2 V_{\text{bulk}}^2 / c^2$ , where  $T_{\text{CMB}} = 2.725\text{K}$ . For reference,  $\sqrt{C_{1,\text{kin}}} \simeq 1(\langle \tau \rangle / 10^{-3})(V_{\text{bulk}} / 100\text{km/sec})\mu\text{K}$ . When computed from the total of  $N_{\text{cl}}$  positions, the dipole will also have positive contributions from 1) instrument noise, 2) the thermal SZ (TSZ) component, 3) the cosmological CMB fluctuation component arising from the last-scattering surface, and 4) the various foreground components within the WMAP frequency range. The last of these contributions can be significant at the lowest WMAP frequencies (channels K & Ka) and, hence, we restrict this analysis to the WMAP Channels Q, V & W which have negligible foreground contributions. The contributions to the dipole from the above terms can be estimated as  $\langle \delta_\nu(\vec{y}) \cos \theta \rangle$  at the  $N_{\text{cl}}$  different cluster locations with polar

angle  $\theta$ . For  $N_{\text{cl}} \gg 1$  the dipole of  $\delta_\nu$  becomes  $a_{1m} \simeq a_{1m}^{\text{kin}} + a_{1m}^{\text{TSZ}} + a_{1m}^{\text{CMB}} + \frac{\sigma_{\text{noise}}}{\sqrt{N_{\text{cl}}}}$ . Here  $a_{1m}^{\text{CMB}}$  is the residual dipole produced at the cluster locations by the primordial CMB anisotropies. The dipole power is  $C_1 = \sum_{m=-1}^{m=1} |a_{1m}|^2$ . The notation for  $a_{1m}$  is such that  $m=0, 1, -1$  correspond to the  $(x, y, z)$  components, with  $z$  running perpendicular to the Galactic plane towards the NGP, and  $(x, y)$  being the Galactic plane with the  $x$ -axis passing through the Galactic center. This dipole signal should not be confused with the "global CMB dipole" that arises from our *local* motion relative to the CMB. The kinematic signal investigated here does not contribute significantly to the "global CMB dipole" arising from only a small number of pixels. When the latter is subtracted from the original CMB maps, only a small fraction,  $\sim (N_{\text{cl}}/N_{\text{total}}) \lesssim 10^{-3}$ , of the kinematic signal  $C_{1,\text{kin}}$  is removed.

The TSZ dipole for a random cluster distribution is  $a_{1m}^{\text{TSZ}} \sim (\langle \tau T_X \rangle / T_{\text{e,ann}}) N_{\text{cl}}^{-1/2}$  decreasing with increasing  $N_{\text{cl}}$ . This decrease could be altered if clusters are not distributed randomly and there may be some cross-talk between the monopole and dipole terms especially for small/sparse samples (Watkins & Feldman 1995), but the value of the TSZ dipole will be estimated directly from the maps as discussed below and in greater detail in Kashlinsky et al (2008 - KA-BKE). The residual CMB dipole,  $C_{1,\text{CMB}}$ , will exceed  $\sigma_{\text{CMB}}^2/N_{\text{cl}}$  because the intrinsic cosmological CMB anisotropies are correlated. On the smallest angular scales in the WMAP data  $\sigma_{\text{CMB}} \simeq 80\mu\text{K}$ , so these anisotropies could be seen as the largest dipole noise source. However, because the power spectrum of the underlying CMB anisotropies is accurately known, this component can be removed with a filter described next.

To remove the cosmological CMB anisotropies we filtered each channel maps separately with the Wiener filter as follows. With the known power spectrum of the cosmological CMB fluctuations,  $C_\ell^{\Lambda\text{CDM}}$ , a filter  $F_\ell$  in  $\ell$ -space which minimizes  $\langle (\delta T - \delta_{\text{instrument noise}})^2 \rangle$  in the presence of instrument noise is given by  $F_\ell = (C_\ell - C_\ell^{\Lambda\text{CDM}})/C_\ell$ , with  $C_\ell$  being the measured power spectrum of each map. Convolving the maps with  $F_\ell$  minimizes the contribution of the cosmological CMB to the dipole. The maps for *each* of the eight WMAP channels were thus processed as follows: 1) for  $C_\ell^{\Lambda\text{CDM}}$  we adopted the best-fit cosmological model for the WMAP data (Hinshaw et al 2007) available from <http://lambda.gsfc.nasa.gov>; 2) each map was decomposed into multipoles,  $a_{\ell m}$ , using HEALPix (Gorski et al 2005); 3) the power spectrum of each map,  $C_\ell$ , was then computed and  $F_\ell$  constructed; 4) the  $a_{\ell m}$  maps were multiplied by  $F_\ell$  and Fourier-transformed back into the angular space  $(\theta, \phi)$ . We then removed the intrinsic dipole, quadrupole and octupole. The filtering affects the effective value of  $\tau$  for each cluster and we calculate this amount later.

Here we use an all-sky cluster sample created by combining the ROSAT-ESO Flux Limited X-ray catalog (REFLEX) (Bohringer et al 2004) in the southern hemisphere, the extended Brightest Cluster Sample (eBCS) (Ebeling et al 1998; Ebeling et al 2000) in the

north, and the Clusters in the Zone of Avoidance (CIZA) (Ebeling et al 2002; Kocevski et al 2007) sample along the Galactic plane. These are the most statistically complete X-ray selected cluster catalogues ever compiled in their respective regions of the sky. All three surveys are X-ray selected and X-ray flux limited using RASS data. The creation of the combined all-sky catalogue of 782 clusters is described in detail by (Kocevski et al 2006) and KA-BKE.

We started with 3-year “foreground-cleaned” WMAP data (<http://lambda.gsfc.nasa.gov>) in each differencing assembly (DA) of the Q, V, and W bands. Each DA is analyzed separately giving us eight independent maps to process: Q1, Q2, V1, V2, W1,..., W4. The CMB maps are pixelized with the HEALPix parameter  $N_{\text{side}}=512$  corresponding to pixels  $\simeq 7'$  on the side or pixel area  $4 \times 10^{-6}$  sr. This resolution is much coarser than that of the X-ray data, which makes our analysis below insensitive to the specifics of the spatial distribution of the cluster gas, such as cooling flows, deviations from spherical symmetry, etc. In the filtered maps for each DA we select all WMAP pixels within the total area defined by the cluster X-ray emission, repeating this exercise for cluster subsamples populating cumulative redshift bins up to a fixed  $z$ . In order to eliminate the influence of Galactic emission and non-CMB radio sources, the CMB maps are subjected to standard WMAP masking. The results for the different masks are similar and agree well within their statistical uncertainties.

The SZ effect ( $\propto n_e$ , the electron density) has larger extent than probed by X-rays (X-ray luminosity  $\propto n_e^2$ ), which is confirmed by our TSZ study using the same cluster catalogue (AKKE). As shown in AKKE, KA-BKE contributions to the TSZ signal are detected out to  $\gtrsim 30'$ . What is important in the present context, is that the X-ray emitting gas is distributed as expected from the  $\Lambda$ CDM profile (Navarro et al 1996) scaling as  $n_e \propto r^{-3}$  in outer parts. In order to be in hydrostatic equilibrium such gas must have temperature decreasing with radius (Komatsu & Seljak 2001). Indeed, the typical polytropic index for such gas would be  $\gamma \simeq 1.2$ , leading to the X-ray temperature decreasing as  $T_X \propto n_e^{\gamma-1} \propto r^{-0.6}$  at outer radii. This  $T_X$  decrease agrees with simulations of cluster formation within the  $\Lambda$ CDM model (Borgani et al 2004) and with the available data on the X-ray temperature profile (Pratt et al 2007). For such gas, the TSZ monopole ( $\propto T_X \tau$ ) decreases faster than the KSZ component ( $\propto \tau$ ) when averaged over a progressively increasing cluster area. To account for this, we compute the dipole component of the final maps for a range of effective cluster sizes, namely  $[1, 2, 4, 6]\theta_{X\text{-ray}}$  and then the maximal cluster extent is set at  $30'$  to avoid a few large clusters (eg. Coma) bias the dipole determination. We note that at the final extent our clusters effectively have the same angular radius of  $0.5^\circ$ . Our choice of the maximal extent is determined by the fact that the SZ signal is detectable in our sample out to that scale (AKKE), which is  $\sim(3-4)$ Mpc at the mean redshift of the sample. Increasing the cluster radius further to  $1^\circ - 3^\circ$ , causes the dipole to start decreasing with the increasing radius, as expected if the pixels outside the clusters are included diluting the KSZ signal (KA-BKE).

To estimate uncertainties in the signal only from the clusters, we use the rest of the map for the distribution and variance of the noise in the measured signal. We use two methods to preserve the geometry defined by the mask and the cluster distribution: 1)  $N_{cl}$  central random pixels are selected outside the mask away from the cluster pixels adding pixels within each cluster’s angular extent around these central random pixels, iteratively verifying that the selected areas do not fall within either the mask or any of the known clusters. 2) We also use a slightly modified version of the above procedure in order to test the effects of the anisotropy of the cluster catalog. There the cluster catalog is rotated randomly, ensuring that the overall geometry of the cluster catalog is accurately preserved. Both methods yield very similar uncertainties; for brevity, we present results obtained with the first method.

## 2. Results

Fig. 1 summarizes our results averaged over all eight DA’s. We find a statistically significant dipole component produced by the cluster pixels for the spheres and shells extending beyond  $z \simeq 0.05$ . It persists *as the monopole component vanishes* and its statistical significance gets particularly high for the  $y$ -component. The signal appears only at the cluster positions and, hence, cannot originate from instrument noise, the CMB or the remaining Galactic foreground components, the contributions from which are given by the uncertainties evaluated from the rest of the CMB map pixels. The signal is restricted to the cluster pixels and thus must arise from the two components of the SZ effect, thermal and/or kinematic.

The TSZ component, however, is given by the monopole term at the cluster positions and cannot be responsible for the detected signal. For the largest apertures it vanishes within the small, compared to the measured dipole, statistical uncertainty, and yet the dipole term remains large and statistically significant. This is the opposite of what one should expect if the dipole is produced by the TSZ component. Any random distribution, such as TSZ emissions, would generate dipole  $\propto \langle \tau T_X \cos \theta \rangle$  which can never exceed (and must be much less than) the monopole component of that distribution,  $\propto \langle \tau T_X \rangle$ . On the other hand, any coherent bulk flow would produce dipole  $\propto V_{bulk} \langle \tau \cos^2 \theta \rangle$ , which is bounded from below by the amplitude of the motion. Furthermore, we find significant dipole from (at least)  $z_{mean}=0.035$  (135 clusters) all the way to  $z_{mean}=0.11$  (674 clusters); its parameters do not depend on the numbers of clusters, pixels used etc. Any dipole component arising from the TSZ term would depend on these parameters as it reflects the (random) dipole of the cluster sample and should thus decrease as more clusters are added in spheres out to progressively larger  $z$ . To verify this, we compute the expected monopole and dipole terms produced by the TSZ effect using the parameters of our cluster catalog as discussed in KA-BKE and recover

the monopole term fairly accurately when the  $\beta$ -profile assumption is reasonable. The TSZ dipole component is then a small fraction of the monopole term. When normalized to the remaining monopole term in Fig. 1a it is completely negligible compared to the measured dipole. Further, the TSZ dipole becomes progressively more negligible as more clusters are added in at higher  $z$ , and its direction varies randomly reflecting the random nature of the intrinsic cluster sample dipole on these large scales. All this is contrary to what we measure.

We thus conclude that the dipole originates from the KSZ effect due to the bulk flow of the cluster sample. Our results indicate a statistically significant bulk-flow component in the final filtered maps for cluster samples in the  $z$ -bins from  $z \leq 0.05$  to  $\leq 0.3$  corresponding to median depth to  $z \simeq 0.1$ , and it also persists when the dipole in shells is computed selecting only clusters at  $z \geq 0.12$  (the median redshift for this sub-sample is  $\simeq 0.18$ ). Fig. 1e shows that the bulk flow results in a CMB dipole with little variation - within the statistical uncertainties - between  $z_{\text{median}} \simeq 0.03$  and  $\gtrsim 0.12$ . The monopole component reflects the residual TSZ contribution which is very small for the maximal cluster aperture as Fig. 1a shows. (At lower  $z$  there may still be some residual TSZ component, which would be consistent with the more nearby clusters having a larger *angular* SZ extent than the more distant ones).

To translate the CMB dipole in  $\mu\text{K}$  into  $V_{\text{bulk}}$  in km/sec, we generated CMB temperatures produced by the KSZ effect for each cluster and estimate the dipole amplitude,  $C_{1,100}$ , contributed by each 100 km/sec of bulk-flow (KA-BKE). The results are shown in the last column of Table 1 of KA-BKE for the central values of the direction of the measured flow; within the uncertainties of  $(l, b)$  they change by at most a few percent. A bulk flow of 100 km/sec leads to  $\sqrt{C_{1,100}} \simeq 1\mu\text{K}$  for unfiltered clusters assuming the  $\beta$ -model; this corresponds to an average optical depth of our cluster sample of  $\langle \tau \rangle \simeq 10^{-3}$  expected for a typical galaxy cluster. For NFW clusters the value of  $C_{1,100}$  would be *smaller*. Filtering reduces the effective  $\tau$  by a factor of  $\simeq 3$ . Since a  $\beta$ -model provides a poor fit to the measured TSZ component outside the estimated values of  $\theta_{\text{X-ray}}$ , we compute  $C_{1,100}$  within that aperture where the central value of the bulk-flow dipole has approximately the same value as at the final apertures. Due to the large size of our cluster sample ( $N_{\text{cl}} \sim 130\text{-}675$ ), the random uncertainties in the estimated values of  $C_{1,100}$  should be small, but we cannot exclude a systematic offset related to selection biases affecting our cluster catalog at high  $z$ . Such offset, if present, will become quantifiable with the next version of our X-ray cluster catalog (in preparation) using the empirically established SZ profile rather than the current  $\beta$ -model to parameterize the cluster TSZ. The good agreement between the various TSZ-related quantities shown in KA-BKE for  $\theta_{\text{SZ}} = \theta_{\text{X-ray}}$  and the observed values for both unfiltered and filtered maps suggests, however, that these systematic uncertainties are likely to be small. They only affect the accuracy of the determination of the amplitude of the bulk flow, but not its existence established by the CMB dipole at the cluster locations. Since the filtering removes  $\tau$  in the

outskirts of clusters more effectively, a larger amount of power is removed in the  $\beta$ -model when the cluster SZ extent is increased beyond  $\theta_{X\text{-ray}}$ , than in the steeper profile measured by AKKE. Thus the effective  $\tau$  is possibly underestimated by using a  $\beta$ -model, but it cannot exceed (and must be much less than) the calibration obtained from the unfiltered  $\beta$ -model.

### 3. Cosmological implications

Conventionally, the entire peculiar velocity field is assumed to be driven by the peculiar gravitational potential. For a given cosmological model, the details of the velocity field also depend on the window function of the dataset. Constructing the precise window function is beyond the scope of this paper, but the overall conclusions would be insensitive to its details because the amplitude and coherence length of the measured flows are quite unexpected within the concordance  $\Lambda$ CDM model. Fig. 1f shows the rms prediction,  $\sigma_V$ , of the concordance  $\Lambda$ CDM model. If produced by gravitational instability within the concordance  $\Lambda$ CDM model, the motion would require the local Universe out to  $\sim 300h^{-1}\text{Mpc}$  to be atypical at the level of many standard deviations of the model. Indeed a value of  $\sqrt{C_{1,100}} \sim 3\mu\text{K}$  is required to reach peculiar velocities of order 100 km/sec on the relevant scales. This is much greater than  $C_{1,100}$  deduced from the *unfiltered* X-ray data and even then it would be difficult to explain the approximate constancy of the measured dipole with depth.

Cosmic variance does not change these conclusions significantly. For a Gaussian density field the peculiar velocity distribution on linear scales is Maxwellian, with the probability density of measuring a 1-D bulk velocity  $p(V)dV \propto V^2 \exp(-1.5V^2/\sigma_V^2)dV$ . The probability of finding a region with  $V < V_0$  is then  $P(V_0) = \Gamma(\frac{3}{2}, \frac{3V_0^2}{2\sigma_V^2})$  where  $\Gamma$  is the incomplete gamma-function normalized to  $\Gamma(n, \infty) = 1$ . The (68%, 95%) c.l. require  $V_0 = (1.08, 1.6)\sigma_V$ ; the shaded area in Fig. 1f shows the 95% c.l. region. In the concordance  $\Lambda$ CDM model  $\sigma_V = (150, 109)$  km/sec at  $(200, 300)h^{-1}\text{Mpc}$ , so 95% of cosmic observers should measure bulk flow velocities less than  $(240, 180)$  km/sec at these scales. To make these numbers consistent with our measurements - at these scales alone - would require  $\sqrt{C_{1,100}} \gtrsim 2\mu\text{K}$ . This is much higher than even the calibration values for unfiltered data (computed for the  $\beta$ -model which leads to a *larger*  $C_{1,100}$  value than the NFW-profile clusters) and cannot be accounted for by any systematic uncertainties in our calibration procedure. Indeed, the distribution of errors is approximately Gaussian (see Fig. 5 of KA-BKE), so the probability of measuring velocity  $V_i \pm \epsilon_i$  at scale  $r_i$  is  $\mathcal{P}_i \propto \int_0^\infty P(V) \exp[-\frac{(V-V_i)^2}{2\epsilon_i^2}]dV$  (e.g. Gorski 1991). The probability of several such independent measurements is the product of  $\mathcal{P}_i$ 's; for the numbers plotted in Fig. 1f this probability is completely negligible. (The measurements in Fig. 1f are not strictly independent since each subsequent  $z$ -bin also contains the clusters from the previous

bin; nevertheless each  $\mathcal{P}_i$  is so small that the overall probability is still negligible).

The coherence length of the measured bulk flow shows no signs of convergence out to  $\gtrsim 300h^{-1}\text{Mpc}$ , and it is quite possible that it extends to much larger scales, possibly all the way across our horizon. An interesting, if exotic, explanation for such a “dark flow” would come naturally within certain inflationary models. In general, within these models the observable Universe represents part of a homogeneous inflated region embedded in an inhomogeneous space-time. On scales much larger than the Hubble radius, pre-inflationary remnants can induce tilt including CMB anisotropies generated by the Grischuk-Zeldovich (Grischuk & Zeldovich 1978) effect (Turner 1991; Kashlinsky et al 1994). These can arise from the parts of space-time that inflated at different times and rates and would manifest themselves mainly in the quadrupole component,  $Q$ : an inhomogeneity of amplitude  $\delta_L \sim 1$  at a distance  $L \gg cH_0^{-1}$  generates a quadrupole  $Q \sim \delta_L(cH_0^{-1}/L)^2$ . Consistency with the observed low value of  $Q$  would require a sufficiently large number of the inflation’s e-foldings, making the Universe flat to within  $|1 - \Omega_{\text{total}}| \leq Q$  and causing the scale of inhomogeneity  $L$  to become comparable to the curvature radius ( $> 500cH_0^{-1}$ ) (Kashlinsky et al 1994). Such a tilted universe would lead to a uniform flow across the observed horizon due to the density gradient produced by this superhorizon mode. The bulk motion would have an amplitude of  $v \sim c\delta_L(cH_0^{-1}/L)$  and would not generate a primordial dipole CMB component (Turner 1991). Since the quadrupole produced by such a pre-inflationary remnant is  $Q \sim (v/c)(cH_0^{-1}/L)$ , it is possible for such inhomogeneities to generate the required motions and be consistent with the observed value of  $Q$  and flatness. Although it would require accidental alignment, the contribution from such an inhomogeneity to CMB anisotropies via the GZ effect might, interestingly, also explain the observed low value of the CMB quadrupole (and possibly also octupole) compared to the concordance  $\Lambda\text{CDM}$  model. This explanation for the measured bulk flow would, however, still require peculiar velocities generated by gravitational instability acting on the  $\Lambda\text{CDM}$  density field, which would provide a random component around the uniform bulk flow. On sufficiently large scales, such a flow would be “cold” in the sense that it would be characterized by a large Mach number (Ostriker & Suto 1990), which may be measurable in future cluster surveys (Atrio-Barandela et al 2004); the Mach number then should increase linearly with scale on scales  $\gtrsim 100h^{-1}\text{Mpc}$ . On smaller scales, there may be non-negligible contributions to the flow from peculiar motions generated by the gravitational instability caused by local matter inhomogeneities. This can lead to a non-alignment with the flow at lower  $z$  in general agreement with the trends in Fig. 1.

This work is supported by NASA ADP grant NNG04G089G and the Ministerio de Educación y Ciencia/”Junta de Castilla y León” in Spain (FIS2006-05319, PR2005-0359 and SA010C05). We thank Gary Hinshaw for useful information on the WMAP data specifics.



## REFERENCES

- Atrio-Barandela, F., Kashlinsky, A., Kocevski, D. & Ebeling, H. 2008, Ap.J. (Letters), 675, L57. (AKKE)
- Atrio-Barandela, F., Kashlinsky, A. & Mucket, J. 2004, Astrophys. J., 601, L111
- Birkinshaw, M. 1999, Phys. Rep., 310, 97-195
- Böhringer, et al. 2004, Astron. Astrophys., 425, 367
- Borgani, S. et al 2004, Mon. Not. R. Astron. Soc., 348, 1078
- Ebeling, H., Edge, A.C., Böhringer, H., Allen, S.W., Crawford, C.S., Fabian, A.C., Voges, W., & Huchra, J.P. 1998, Mon. Not. R. Astron. Soc., 301, 881
- Ebeling, H., Edge A.C., Allen S.W., Crawford C.S., Fabian A.C., & Huchra J.P. 2000, Mon. Not. R. Astron. Soc., 318, 333
- Ebeling, H., Mullis, C.R., & Tully R.B. 2002, Astrophys. J, 580, 774
- Gorski, K. et al 2005, Astrophys. J., 622, 759
- Gorski, K. 1991, Ap.J., 370, L5
- Grishchuk, L. & Zeldovich, Ya.B. 1978, Sov. Astron., 22, 125
- Hinshaw, G. et al 2007, Astrophys. J., 170, 288
- Kashlinsky, A., Tkachev, I., Frieman, J. 1994, Phys. Rev. Lett., 73, 1582
- Kashlinsky, A. & Atrio-Barandela, F. 2000, Astrophys. J., 536, L67 (KA-B)
- Kashlinsky, A., Atrio-Barandela, F., Kocevski, D. & Ebeling, H. 2008, Ap.J., submitted. (KA-BKE)
- Kashlinsky, A. & Jones, B.J.T. 1991, Nature, 349, 753
- Kocevski, D.D., Mullis, C.R., & Ebeling, H. 2004, Astrophys. J., 608, 721
- Kocevski, D.D. & Ebeling, H. 2006, Astrophys. J., 645, 1043
- Kocevski, D.D., Ebeling, H., Mullis, C.R., & Tully, R.B. 2007, Astrophys. J., *in press*
- Komatsu, E. & Seljak, U. 2001, Mon. Not. R. Astron. Soc., 327, 1353

Navarro, J.F., Frenk, C.S. & White, S.D.M. 1996, *Astrophys. J.*, 462, 563

Ostriker, J. & Suto, Y. 1990, *Astrophys. J.*, 348, 378

Pratt, G. et al 2007, *Astron. Astrophys.* 461, 71

Strauss, M. & Willick, J.A. 1995, *Phys. Rep.*, 261, 271

Turner, M. S. 1991, *Phys.Rev.*, 44, 3737

Watkins, R. & Feldman, H. A. 1995, *Astrophys. J.*, 453, L73

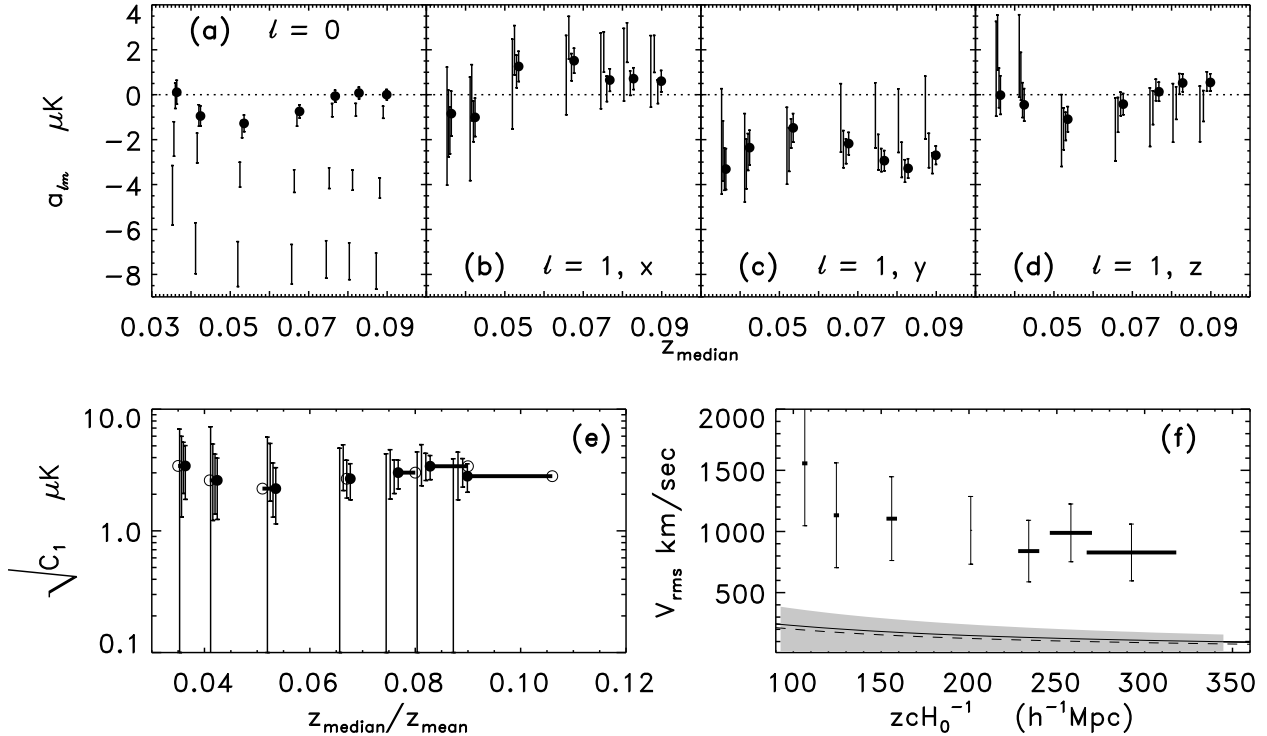


Fig. 1.— **Upper panels:** (a)-(d) Monopole and dipole terms for  $\theta_{SZ} = \min[(1, 2, 4, 6) \times \theta_{X\text{-ray}}, 30']$  with  $1\text{-}\sigma$  standard deviations. Values at the maximal aperture, which have the lowest monopole term, are marked with filled circles. The averaged monopole and dipole components are weighted with statistical uncertainties. The statistical significance of the KSZ component improves as more of the cluster pixels producing the signal are included at higher  $z$ . The noise of our measurement of the dipole at  $1.8(N_{cl}/100)^{-1/2}\mu\text{K}$  with three-year WMAP data is in good agreement with the expectations of KA-B. **Lower panel.** (e) - Outer  $z$ -bins with signal measured at  $\gtrsim 2\sigma$ . Filled circles show the values from Table 1 of KA-BKE at the maximal aperture vs the median  $z$ ; open symbols show the same vs the mean  $z$ . The two symbols are connected to show the uncertainty in the scale on which the flow is probed. Signal recovered at  $\theta_{SZ} = \min[(1, 2, 4) \times \theta_{X\text{-ray}}, 30']$  is shown with  $1\sigma$  error bars; from left to right in order of increasing aperture. The values are slightly displaced around the true  $z_{\text{median}}$  for clearer display. (f) - Comparison between theoretically expected bulk flow and the measurements. The rms bulk velocity for the concordance  $\Lambda\text{CDM}$  model which best fits the WMAP 3-year data for top-hat (solid line) and Gaussian (dashes) windows; shaded region marks the 95% cl from cosmic variance. The results of this study, translated into km/sec using  $\sqrt{C_{1,100}} = 0.3\mu\text{K}$ , are shown with  $1\text{-}\sigma$  errors vs the mean/median redshift of the clusters in each cumulative  $z$ -bin. The horizontal bars connect  $z_{\text{mean}}$  with  $z_{\text{median}}$ . The results in shells from Table 1 in KA-BKE are omitted in this comparison because of the theoretical windows plotted, but they show that the motion extends to mean redshift  $\gtrsim 0.18$  well beyond the horizontal range of the figure.